

Collagen Composition and Content-Dependent Contrast in Porcine Annulus Fibrosus Achieved by Using Double Quantum and Magnetization Transfer Filtered UTE MRI

Uzi Eliav,¹ Michal E. Komlosh,^{2,3} Peter J. Basser,² and Gil Navon^{1*}

Purpose: To test the potential of combining double quantum and magnetization transfer filtered ultra-short echo time (DQF-MT-UTE) MRI to obtain information about the macromolecular composition and characteristics of connective tissues.

Methods: A DQF-MT-UTE pulse sequence was implemented on a 14.1 T AVANCE III Bruker spectrometer equipped with a Bruker micro2.5-imaging gradient system to obtain images of porcine annulus fibrosus.

Results: The DQF-MT-UTE MRI of the annulus fibrosus of porcine intervertebral disc, where the creation time of the double quantum coherence filtering (DQF) was on a time scale appropriate for excitation of macromolecules, showed stronger signal from the outer layers of the disc than from the inner layers closer to the nucleus pulposus. Similarly, spectroscopic studies showed the same trend in the efficiency of the magnetization transfer (MT) from collagen to water.

Conclusion: DQF-MT filtered UTE MRI of the annulus fibrosus provides new contrast parameters that depend on the concentration of the collagen and on the rate and efficiency of MT of its protons to water. The latter parameters appear to be different for collagen types I and II in the annulus fibrosus. **Magn Reson Med 000:000–000, 2013. © 2013 Wiley Periodicals, Inc.**

Key words: intervertebral disc; annulus fibrosus; collagen type I; collagen type II; double quantum filter; magnetization transfer; ultra-short TE

Magnetic resonance imaging (MRI) of connective tissues has been hampered by the short T_2 that results from interactions of water molecules with collagen fibers. The development of ultra-short time-to-echo (UTE) MRI technique has enabled the observation of these tissues with improved signal-to-noise ratio and alleviated the problem of the magic angle artifacts (1–4). However, the homogeneous

image in connective tissues obtained with these techniques belies the heterogeneous nature of the macromolecules within the tissue. In a previous work (5) it was shown that by combining UTE with double quantum (DQ) and magnetization transfer (MT) filtering (DQF-MT-UTE, see Fig. 1) (6–8), it was possible to obtain contrast between tissue compartments based on the following characteristics: (a) the residual dipolar coupling interaction within the biomacromolecules (bioMM) (6,7), which depends on their structure; (b) residual dipolar interactions within the water molecules (8–10); and (c) the magnetization exchange rate between bioMM and water (6,7). Using this combination of methods, it was demonstrated that, in rat tail specimens, significant contrast, based on the macromolecular characteristics differences between tendons and annulus fibrosus. This contrast was interpreted as reflecting differences in macromolecular composition. However, due to limited spatial resolution this hypothesis could not be tested experimentally in the annulus fibrosus of the rat tail. In the current study, we have used the much larger porcine annulus fibrosus to examine the effects of the bioMM composition and distribution within this tissue and of water interactions with the bioMM on the observed contrast using the DQF-MT-UTE method.

As mentioned above the DQF-MT-UTE method distinguishes between molecules on the basis of differences in their dipolar interactions and their molecular dynamics. For collagen in connective tissues such as tendon where the motions are slow or anisotropic the size of the dipolar interactions between protons are in the range of tens of kHz (6,7). On the other hand, for bioMM-associated water molecules the intramolecular dipolar interactions are significantly reduced as a result of their fast isotropic or slightly anisotropic reorientational motion and various exchange processes (8–10). For water, typical residual dipolar interactions are less than 1 kHz.

We use DQF-MT-UTE MRI (5) (Fig. 1) to study the effects of the residual dipolar interaction in tissues. By examining the dependence on the creation/reconversion time interval τ (5) (Fig. 1). It was shown to provide information about the collagen protons (5) while the dependence on the exchange time interval t_{LM} (Fig. 1) enabled the measurement of MT rates of bioMM protons to water protons (For details, see Refs. 5–8).

METHODS

¹H-MRI experiments were conducted on a 14.1 T AVANCE III Bruker spectrometer equipped with a Bruker

¹School of Chemistry, Tel Aviv University, Tel Aviv, Israel.

²Section on Tissue Biophysics and Biomimetics (STBB), Eunice Kennedy Shriver National Institute of Child Health and Human Development (NICHD), NIH, Bethesda, Maryland, USA.

³Center for Neuroregenerative Medicine (CNRM) and the Henry Jackson Foundation (HJF), Bethesda, Maryland, USA.

Grant sponsor: US-Israel Binational Science Foundation; Grant number: 2007157; Grant sponsor: European FP7 program ENCITE; Grant sponsor: Israel Ministry of Science and Technology; Grant number: 3–6446; Grant sponsors: Intramural Program of the Eunice Kennedy Shriver National Institute of Child Health and Human Development, Center for Regenerative Medicine within the US Department of Defense.

*Correspondence to: G. Navon, Ph.D., School of Chemistry, Tel Aviv University, Haim Levanon Street, Tel Aviv, 69978, Israel. E-mail: navon@post.tau.ac.il

Received 27 August 2012; revised 19 December 2012; accepted 8 January 2013

DOI 10.1002/mrm.24662

Published online 00 Month 2013 in Wiley Online Library (wileyonlinelibrary.com).

© 2013 Wiley Periodicals, Inc.

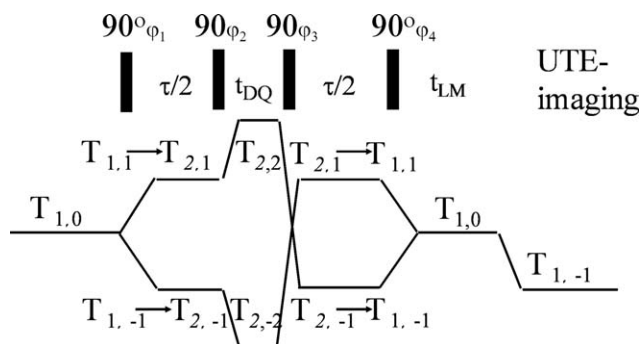


FIG. 1. DQF-MT weighted UTE imaging pulse sequence (5,6). The hard 90° pulses shown in Figure 1 were 14–17 μs .

micro2.5-imaging gradient system with a nominal gradient strength of $24.65 \text{ mT m}^{-1} \text{ Amp}^{-1}$ and Bruker GREAT 60 gradient amplifiers. Spectroscopic studies were also carried out on an AVANCE WB 8.4T Bruker spectrometer equipped with a Bruker micro5 microimaging probe. All r.f. coils used on the 14.1 T AVANCE III spectrometer were birdcage while on the AVANCE WB 8.47 T they were saddle coils. The pulse sequence shown in Figure 1 was used with commercially available 2D ultra-short TE pulse sequence (Bruker). For spectroscopy, the MRI module was replaced by a single 90° pulse.

MATERIALS

The combined DQF and UTE MRI experiments were performed on porcine annulus fibrosus. These were harvested within a few hours after the animal was sacrificed and used without any delay. For the imaging experiments, the annulus fibrosus was cut into two pieces (for an illustration, see Fig. 2 regions marked Ai and Bi), one from its outer layer and the other from its inner layer (close to the nucleus pulposus). These pieces were placed one on top of another in a homemade 10-mm diameter cylindrical vessel consisting of two compartments made of UltemTM (Polyetherimide Ensinger, UK). The sample vessel was filled with perfluoropolyether (Fomblin LC/8, Solvay Solexis, Italy) to further reduce susceptibility artifacts. The MRI experiments were repeated twice with freshly prepared samples while the spectroscopic studies were performed on five pairs of specimen excised from the outer and inner layers of the porcine annulus fibrosus (marked as A_s and B_s in Fig. 2). Each of these pieces was measured separately.

RESULTS

The three images in Figure 3b–d demonstrate the dependence of DQF-MT weighted MRIs of porcine annulus fibrosus on the creation/reconversion time, $\tau/2$, while the exchange time t_{LM} was kept constant (200 ms, see the last two paragraphs in the current section describing the MT process where this particular choice is explained). In the upper row of Figure 3, we present a UTE image (i.e., without DQF-MT weighting). In all the images the upper piece shows the outer layer of the tissue, while the lower piece

shows the inner layer. The UTE MRI that was done on the time scale of time to echo (TE) ~ 0.2 ms had homogeneous image intensity and was not affected by the water T_2 . This result is expected since the T_2 of the porcine annulus fibrosus was found in a previous study to be in the range of 25–50 ms (11). Thus, the UTE image intensity reflects the proton densities of water, and to a lesser extent of proteoglycans, which constitute only 2–5% of the annulus fibrosus dry weight (12). On the other hand, it is noteworthy that in the DQF-MT-UTE images (Fig. 3b–d), the intensity of the signal declines from the outer to inner layers of the annulus fibrosus. Repeating DQF-MT weighted UTE MRI on another sample gave similar results.

To better understand and quantify this behavior in the annulus fibrosus, the outer (region Ai in Fig. 2) and the inner (region Bi in Fig. 2) layers were divided into four sub-regions (sub-regions A–D, Fig. 3a) and the average intensities of the images (such as shown in Fig. 3b–d) measured as a function of the creation/reconversion time, $\tau/2$ was calculated, using Bruker's built in software (Fig. 3e). These curves were fit to a Gaussian decay function plus a constant (Eq. [1]) that approximate an initial signal buildup due to the water intramolecular dipolar interaction (More detailed information about this phenomenon is given below in the discussion associated with Fig. 4).

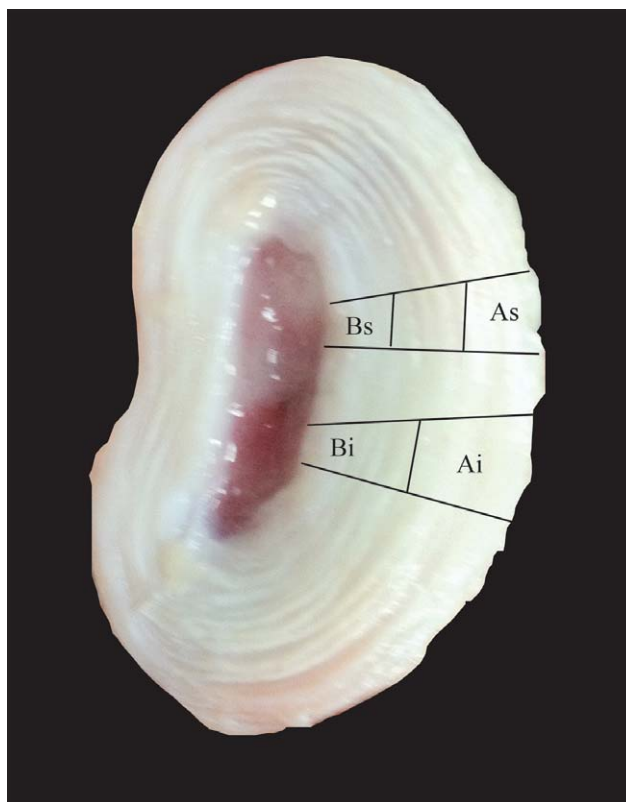


FIG. 2. A photo of an axial section of porcine annulus fibrosus where the regions extracted for imaging and spectroscopy are marked as Ai and Bi and As and Bs, respectively.

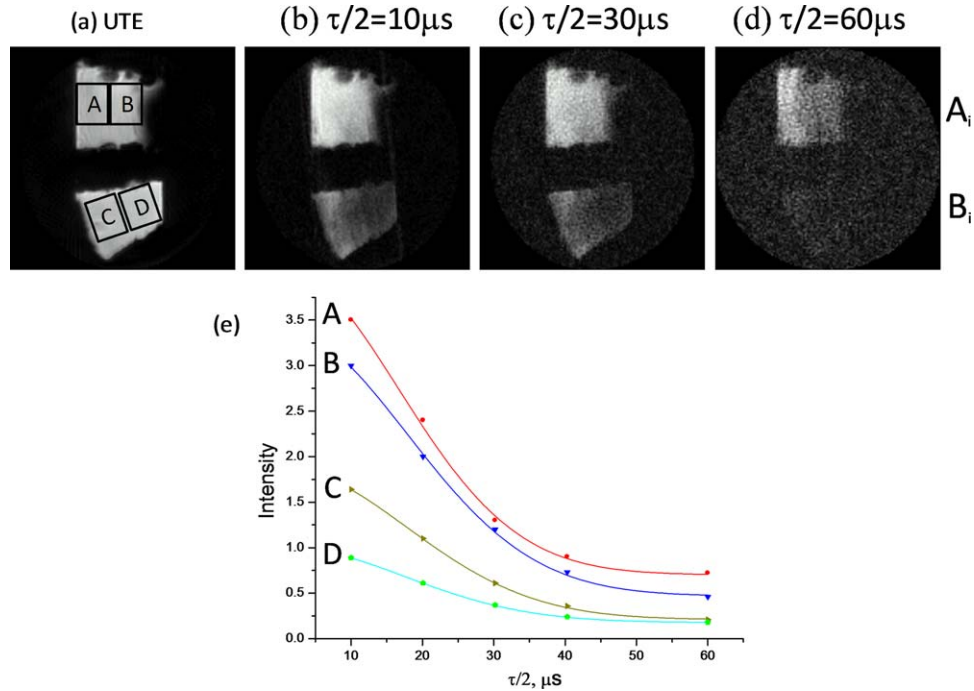


FIG. 3. MR images obtained by DQF-MT/UTE with $t_{LM} = 200$ ms. The pieces were placed so that the right-most part of each of them is facing the nucleus pulposus; the two pieces of the annulus fibrosus in Figure 2 that are marked as A_i and B_i were placed in the upper and lower parts of the sample vessel. The images in (b–d) demonstrate the dependence on the creation/reconversion time, $\tau/2$, while the image in (a) was obtained by a commercially available UTE method. Imaging details: TE = 0.27 ms, repetition time (TR) = 5 s, slice thickness = 1 mm, field of view (FOV) = 1.5 cm, Matrix size = 128×128 . Fitting of the decays of DQF-MT weighted MRIs of the annulus fibrosus as a function of the creation/reconversion time, $\tau/2$, to a gaussian with constant (Eq. [1], full curves) are shown. Symbols represent experimental data. For all regions (A–D) t_{decay} was 34 ± 2 μs . [Color figure can be viewed in the online issue, which is available at wileyonlinelibrary.com.]

$$A \exp(-2(\tau/2t_{decay})^2) + C \quad [1]$$

The choice of gaussian is based on our previous observation of the lineshape of collagen in tendon (6). Such lineshape is consistent with the fact that in solids, where there is a dispersion of dipolar interactions, the lineshape is commonly described as gaussian. Collagen is rigid, particularly when embedded in fibrils, and exhibits a dispersion of dipolar interactions, thus conforming to the fitting requirements above.

As can be seen from the curves shown in Figure 3e, all sub-regions of the annulus fibrosus have a very short decay time constant (see the caption of Fig. 3), which suggests that we are observing protons in rigid bioMMs such as collagen, and not in flexible bioMMs such as proteoglycans (13). The similarity of the decay times of all sub-regions reduces the possibility that the collagen spin dynamics throughout the sample are responsible for the observed contrast in the DQF-MT-weighted UTE experiment. It should be noted that though the decay times are similar they differ by their initial intensity and by the contribution of the signal build up due to the water intramolecular dipolar interaction. Thus, the source of the contrast must be the variation in the amounts of the collagen, or the efficiency of MT to the water, or a combination of the two. Indeed, the amount of collagen is known to decline radially, toward the inner layer of the annulus fibrosus (12). However,

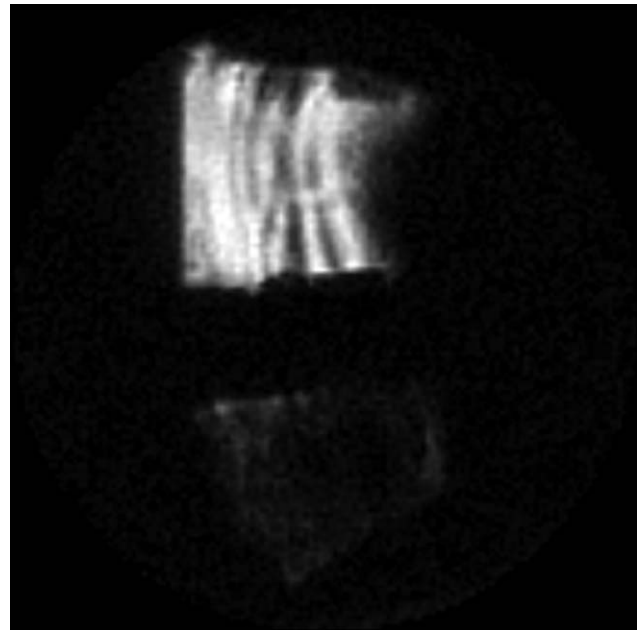


FIG. 4. DQF-MT weighted UTE MRIs obtained for $\tau/2 = 1.4$ ms and $t_{LM} = 2$ μs . The left side of the upper and right side of the lower pieces are the outer and inner layers of the annulus fibrosus, respectively. Under these conditions, the intramolecular dipolar interaction of the water dominates the image intensity. Imaging details: TE = 0.27 ms, TR = 5 s, slice thickness = 1 mm, FOV = 1.5 cm, matrix size = 128×128 .

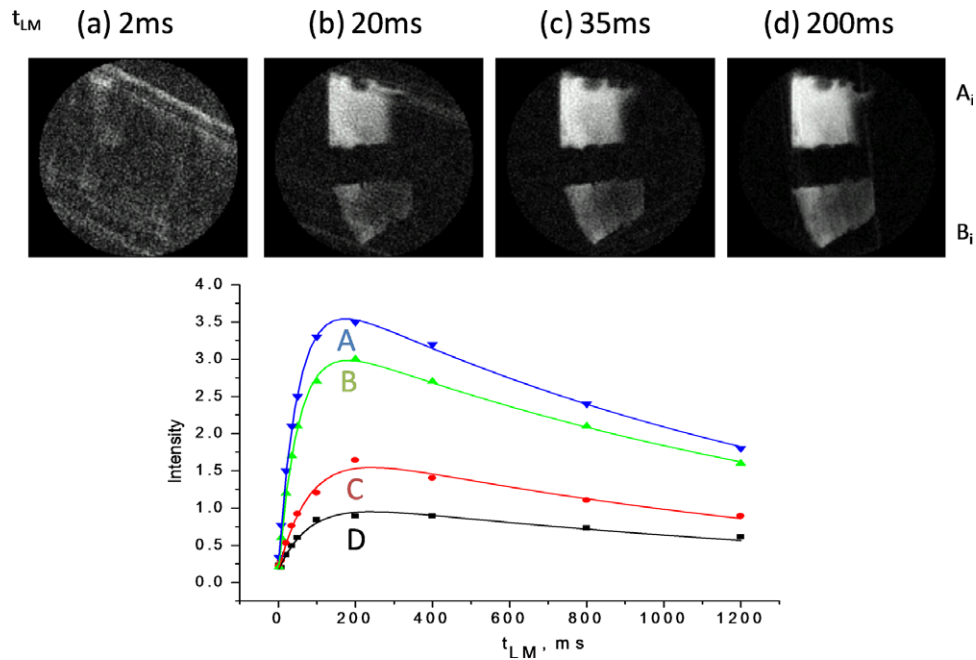


FIG. 5. Dependence of porcine annulus fibrosus images on MT period t_{LM} for $\tau/2 = 10 \mu\text{s}$ (a–d). The decay of average intensities of regions of the DQF-MT weighted UTE images of the annulus fibrosus shown in (e) as a function of the MT period, t_{LM} , (see Fig. 1) fit to a bi-exponential decay (solid curves). Symbols represent the experimental data. (A) Region A in Figure 3 with $t_{rise} = 50 \text{ ms}$, (B) region B in Figure 3 with $t_{rise} = 50 \text{ ms}$, (C) region C in Figure 3 with $t_{rise} = 80 \text{ ms}$, (D) region D in Figure 3 with $t_{rise} = 80 \text{ ms}$. Imaging details: TE = 0.27 ms, TR = 5 s, slice thickness = 1 mm, FOV = 1.5 cm, matrix size = 128×128 . [Color figure can be viewed in the online issue, which is available at wileyonlinelibrary.com.]

the degree of the decline, which is about a factor of two, cannot account for the much larger decline in intensity of about a factor of four apparent here (Fig. 3e). This decline must be also due to differences in the efficiency of MT to the water in the various parts of the annulus fibrosus. Preliminary spectroscopic studies showed that the percentage of collagen magnetization transferred to the water is 0.72 and 0.35 (averaged over several samples) in the outer (region A_s in Fig. 2) and the inner (region B_s in Fig. 2) layers of the annulus, respectively. These efficiencies of magnetization transfer are calculated using the ratio of the integrals of the spectra measured with $t_{LM} = 10 \mu\text{s}$ and spectral range of 100 kHz (only collagen spectrum is observed) and 200 ms and spectral range of 1 kHz (where maximum transfer to water is observed). Though, the figures for the MT efficiency were found to vary significantly among different samples (as much as $\pm 35\%$) the ratio of transfer efficiencies of about two between the outer and inner layers for a given sample remains constant.

Under the conditions of long creation/reconversion time (i.e., $110 \mu\text{s} \leq \tau/2 \leq 1400 \mu\text{s}$ and $t_{LM} \leq 2 \text{ ms}$), the collagen magnetization has completely decayed away and the observed signal results from the formation of second rank tensors due to the intramolecular residual dipolar interaction of water molecules exchanging with water molecules bound to the collagen (5,8). A typical contrast of this type is shown in Figure 4 for $\tau/2 = 1,400 \mu\text{s}$ and $t_{LM} = 2 \mu\text{s}$. As seen from the image, the signal in the outer layer (region A_i in Fig. 2) is stronger than in the inner layer (region B_i in Fig. 2) by a factor of 15.

This factor cannot be accounted for only by the 2-fold ratio in the collagen content of the two layers. The reason for this is that such a ratio implies factor of two in the residual dipolar interaction and thus a factor of up to four in the intensity ratio between the two layers. As is further discussed in the discussion section, the larger ratio of 15 in the intensity may be a result of the faster proton exchange between water molecules in the inner layer.

To verify that the images shown in Figure 3 are the result of MT from the collagen to the water and that there are differences in the MT rates on moving from the outer to inner layer of the annulus fibrosus, we obtained these images as a function of the MT period, t_{LM} , while keeping the creation/reconversion, $\tau/2$, very short (10 μs). The results are shown in Figure 5a–d. For $t_{LM} \leq 2 \text{ ms}$ no image is obtained. The image intensity increases with increasing t_{LM} going through a maximum at $t_{LM} = 200 \text{ ms}$ and then decaying as a result of T_1 at long t_{LM} (5–7). Therefore, magnetization exchange time of $t_{LM} = 200 \text{ ms}$ was chosen to study the signal dependence on the creation/reconversion time $\tau/2$. Furthermore, previous studies have shown that the signal maximum is independent of the MT rate (6,7) and thus it was of interest to study the dependence on creation/reconversion time $\tau/2$ at this t_{LM} value. On the basis of discussion above of the results shown in Figures 3 and 5, we can conclude that the images are derived from water magnetization that originates from the collagen. An analysis of the dependence of the average intensity of the four regions (A–D, Fig. 3a) of the annulus fibrosus

on the MT period t_{LM} is shown on the bottom line of Figure 5. The data were fitted to a difference of two exponentials (Eq. [2]).

$$A(\exp(-t_{LM}/T_1) - \exp(-t_{LM}/t_{rise})) \quad [2]$$

The decay rates were found to be approximately 1.5 s, consistent with the values of T_1 that were observed for collagen in tendons (5,6). On the other hand, the buildup time constant, t_{rise} , of the inner layer (~ 80 ms) was longer than that of the outer layer (~ 51 ms). This slower rate of the MT from the inner layer to water is consistent with the lower efficiency of this process we measured in this layer. Both effects, the slower rate of MT and the lower efficiency of this process, may have a common origin and may be a characteristic of collagen type II, which is the major component in the inner layer, as compared to collagen type I, which is the major component in the outer layer.

DISCUSSION

In order to account for the contrast observed in the images shown in Figure 3 and 5 the results above show that it is necessary to account for variations in collagen content as well as the efficiency of MT between the collagen and water. On the other hand, the contrast in Figure 4 is not related directly to the amount of collagen but rather to the fraction of bound water molecules. This parameter may also help explain the variations in the efficiency of the MT between the collagen and water. The variations in the fraction of bound water molecules can be the result of the changes in the type of collagen in the various regions of the annulus fibrosus. For instance, it is known that the amount of collagen type II increases and the amount of collagen type I decreases from the outside of the intervertebral disc toward the nucleus pulposus (14,15). Consistent with the above interpretation are ^2H studies of D_2O in cartilage, where it was shown that residual quadrupolar interactions of deuterium in the radial zone of articular cartilage (~ 400 Hz) (16) are much smaller than in tendon ($\sim 2,700$ Hz) (8), indicating weaker binding of water in the cartilage. Such weaker binding of the water to collagen type II is likely to decrease the efficiency of MT from the collagen to the water.

The effects of the proteoglycans in the cartilage, tendon, and the annulus fibrosus should also be considered. The relative amounts of proteoglycans are larger in cartilage than in tendon; in disc tissue they also increase from the outer to the inner layers of the annulus and, therefore, could have an effect on water binding to the collagen. However, in a previous ^2H -DQF study of D_2O in articular cartilage, the water ^2H quadrupolar splitting, resulting from the interaction between water and the collagen fibers, was not affected by proteoglycan degradation with trypsin (16), thus indicating that proteoglycan does not play a significant role in the binding of water molecules to collagen. It is worth noting that the T_2 in the porcine annulus fibrosus increases from the outer (~ 25 ms) to the inner layers (~ 50 ms) of the tissue (11). This change is consistent with the interpretation of the

results given in Figure 4, i.e., that a decline in the fraction of water bound to the collagen and the reduction of the water intramolecular residual dipolar interaction, which may be associated to the transition from type I to type II collagen. However, though proteoglycans may not affect the percentage of binding to the collagen they still can have an effect on the image in Figure 4 since they may cause the exchange rates among the water molecules, k , to increase from the outer to the inner parts of the annulus fibrosus following the increase of proteoglycan concentration in this direction (15). Since for exchange rates larger than the residual dipolar interaction the DQF-MT signal intensity is proportional to $1/k^2$ (8) the increase of k should result in a decrease of the signal intensity. This effect was previously demonstrated experimentally by changes of temperature (8), pH (Eliav, Seo and Navon, unpublished results), and buffer concentration (17).

CONCLUSION

DQF-MT weighted UTE MRI of the annulus fibrosus provides new contrast parameters that depend on the concentration of the collagen and on the rate and efficiency of MT of its protons to water. The latter parameters appear to be different for collagen types I and II in the annulus fibrosus. In that case the present study could become the basis of a non-invasive MRI method for collagen typing. Both the differences in the efficiency of the MT between the collagen and water and the water residual dipolar interaction seem to be related to differences in the fractions of the water molecules bound to the collagen.

ACKNOWLEDGMENTS

Authors are grateful to Mrs. Joni Taylor, Mr. Timothy Hunt, and Mr. David Chess from NHLBI for obtaining the specimen. They are also thankful to Dr. Galit Saar from LFMI/NINDS, for her help with the sample preparations, and to Dr. Doug Morris from the NMRF/NINDS for assisting with the 14T MRI instrumentation.

REFERENCES

1. Robson MD, Gatehouse PD, Bydder M, Bydder GM. Magnetic resonance: an introduction to ultrashort TE (UTE) imaging. *J Comput Assist Tomogr* 2003;27:825–846.
2. Robson MD, Bydder GM. Clinical ultrashort echo time imaging of bone and other connective tissues. *NMR Biomed* 2006;19:765–780.
3. Fullerton GD, Cameron IL, Ord VA. Orientation of tendons in magnetic field and its effect on T2 relaxation-times. *Radiology* 1985;155:433–435.
4. Du J, Pak BC, Znamirowski R, Statum S, Takahashi A, Chung CB, Bydder GM. Magic angle effect in magnetic resonance imaging of the Achilles tendon and entheses. *Magn Reson Imaging* 2009;27:557–564.
5. Eliav U, Komlosch EM, Basser, PJ and Navon G. Characterization and mapping of dipolar interactions within macromolecules in tissues using combination of DQF, MT and UTE MRI. *NMR Biomed* 2012;25:1152–1159.
6. Eliav U, Navon G. Multiple quantum filtered NMR studies of the interaction between collagen and water in the tendon. *J Am Chem Soc* 2002;124:3125–3132.
7. Neufeld A, Eliav U, Navon G. New MRI method with contrast based on the macromolecular characteristics of tissues. *Magn Reson Med* 2003;50:229–234.
8. Eliav U, Navon G. A study of dipolar interactions and dynamic processes of water molecules in tendon by H-1 and H-2 homonuclear and

- heteronuclear multiple-quantum-filtered NMR spectroscopy. *J Magn Reson* 1999;137:295–310.
9. Migchels C, Berendsen HJ. Proton exchange and molecular orientation of water in hydrated collagen fibers—NMR-study of H₂O and D₂O. *J Chem Phys* 1973;59:296–305.
 10. Kalk A, Berendsen HJC. Proton magnetic-relaxation and spin diffusion in proteins. *J Magn Reson* 1976;24:343–366.
 11. Saar G, Zhang B, Ling W, Regatte RR, Navon G, Jerschow A. Assessment of glycosaminoglycan concentration changes in the intervertebral disc via chemical exchange saturation transfer. *NMR Biomed* 2012;25:255–261.
 12. Adams P, Eyre DR, Muir H. Biochemical aspects of development and ageing of human lumbar intervertebral discs. *Reumatol Rehabil* 1977;16:22–29.
 13. Naji L, Kaufmann J, Huster D, Schiller J, Arnold K. ¹³C NMR relaxation studies on cartilage and cartilage components. *Carbohydr Res* 2000;327:439–446.
 14. Grynblas MD, Eyre DR, Kirschner DA. Collagen type-II differs from type-I in native molecular packing. *Biochim Biophys Acta* 1980;626:346–355.
 15. Eyre DR, Muir H. Type-1 and Type-2 collagens in intervertebral-disk—interchanging radial distributions in annulus fibrosus. *Biochem J* 1976;157:267–270.
 16. Keinan-Adamsky K, Shinar H, and Navon G. The effect of detachment of the articular cartilage from its calcified zone on the cartilage microstructure, assessed by H-spectroscopic double quantum filtered MRI. *J Orthop Res* 2005;23:109–117.
 17. Zheng SK, Xia Y. Effect of phosphate electrolyte buffer on the dynamics of water in tendon and cartilage. *NMR Biomed* 2009;22:158–164.